

# Optical studies of ZnS:Mn films grown by pulsed laser deposition

K. M. Yeung, W. S. Tsang, C. L. Mak,<sup>a)</sup> and K. H. Wong

*Department of Applied Physics and Materials Research Center, The Hong Kong Polytechnic University, Hung Hom, Hong Kong SAR, China*

(Received 22 April 2002; accepted for publication 2 July 2002)

High-quality ZnS:Mn thin films have been deposited on (001)Si substrates at various temperatures using pulsed laser deposition. Their structural properties were characterized by x-ray diffraction. Optical studies by spectroscopic ellipsometry, optical transmittance, and photoluminescence measurements were systematically carried out on all film samples. In the analysis of the measured SE spectra, a modified double-layer Sellmeier model was adopted to represent the optical properties of the ZnS:Mn films. In this model, the films were assumed to consist of two layers—a bottom bulk ZnS:Mn layer and a surface layer composed of bulk ZnS:Mn as well as void. Good agreement was obtained between the measured spectra and the model calculations. Changes in the refractive indices of the ZnS:Mn films as a function of growth temperature were investigated. The PL and absorption measurements revealed that the orange-yellow emission band at  $\sim 590$  nm and the absorption edge at  $\sim 370$  nm upshifted to shorter wavelengths for films deposited at higher substrate temperatures. These results imply that the energy gap of the ZnS:Mn films increases with growth temperature. The observed changes of optical properties in these films are correlated to their structural qualities.

© 2002 American Institute of Physics. [DOI: 10.1063/1.1503389]

## I. INTRODUCTION

Zinc-sulfide (ZnS) thin films have received much attention due to their wide applications in electroluminescent (EL) devices. Various techniques, such as sputtering,<sup>1</sup> metal-organic chemical vapor deposition,<sup>2</sup> molecular beam epitaxy,<sup>3</sup> atomic layer epitaxy,<sup>4</sup> sol-gel,<sup>5</sup> spray pyrolysis,<sup>6</sup> physical vapor deposition,<sup>7</sup> and pulsed laser deposition (PLD),<sup>8,9</sup> have been employed to prepare ZnS films. Among them, PLD is a recognized method, best known for its low substrate-heating requirement, ability to retain the film stoichiometry, fast deposition rate, and simple setup.

In this study, high quality ZnS:Mn films were fabricated on (001)Si and ITO-coated glass substrates by PLD method. Effects of the deposition temperature on the optical and structural properties of these ZnS:Mn films were investigated. The output properties of thin film electroluminescent (EL) devices significantly depend on the optical efficiency of the phosphor layer. In order to obtain a more precise measurement on the efficiency, detailed analysis of the radiation patterns should be taken into account. Recently, Richter and Mauch<sup>10</sup> showed that the scattering gain could help to understand the optical properties of inverted EL structures. The performance of the phosphor films also depends on the optical constant. For example, in thin film EL devices, if the ZnS:Mn (phosphor) layer is sandwiched between insulating layers of smaller refractive indices, a large part of EL emission from the phosphor layer is trapped within the same layer due to total internal reflection. Therefore, the refractive index of ZnS:Mn films is an importance factor in controlling the output luminance of EL devices.<sup>11</sup>

Spectroscopic ellipsometry (SE) is a nondestructive testing technique using light reflection. In conjunction with computer modeling, SE is capable of angstrom-level depth profiling and optical characterization of thin films. Generally, SE measures the traditional ellipsometric angles,  $\psi$  and  $\Delta$ , as functions of energy in the experiment. However, in this study, a spectroscopic phase modulated method was used.<sup>12</sup> The incident light beam was polarized before reflecting from the sample. The reflected beam, after passing through a photoelastic modulator ( $M$ ) and an analyzer ( $A$ ), was dispersed by a monochromator and detected by a photomultiplier tube. The orientations (with respect to the plane of incidence) of the polarizer, modulator and analyzer are denoted  $P$ ,  $M$ , and  $A$ , respectively. The photoelastic modulator consisted of a fused silica block sandwiched between piezoelectric quartz crystals oscillating at a frequency of  $\sim 50$  kHz. This generated a periodic phase shift  $\delta(t)$  between orthogonal amplitude components of the transmitted beam. The detected intensity, in this case, would take the general form:<sup>12</sup>

$$I(t) = I[I_0 + I_S \sin \delta(t) + I_C \cos \delta(t)], \quad (1)$$

where  $I$  is a constant, and

$$\begin{aligned} I_0 &= 1 - \cos 2\psi \cos 2A + \cos 2(P-M) \cos 2M (\cos 2A \\ &\quad - \cos 2\psi) + \sin 2A \cos \Delta \cos 2(P-M) \sin 2\psi \sin 2M \\ I_S &= \sin 2(P-M) \sin 2A \sin 2\psi \sin \Delta \\ I_C &= \sin 2(P-M) [\sin 2M (\cos 2\psi - \cos 2A) \\ &\quad + \sin 2A \cos 2M \sin 2\psi \sin \Delta]. \end{aligned} \quad (2)$$

For a suitable choice of angle  $A$ ,  $M$ , and  $P$ , a simple determination of the ellipsometric angles from  $I_0$ ,  $I_S$ , and  $I_C$  could be obtained. Throughout the experiment, we set

<sup>a)</sup> Author to whom correspondence should be addressed; electronic mail: apaclmak@polyu.edu.hk

$$P - M = +45^\circ; M = 0^\circ; \text{ and } A = +45^\circ, \quad (3)$$

so that

$$\begin{aligned} I_0 &= 1 \\ I_S &= \sin 2\psi \sin \Delta, \\ I_C &= \sin 2\psi \cos \Delta, \end{aligned} \quad (4)$$

therefore, we could calculate  $\psi$  and  $\Delta$  accurately by obtaining  $I_S$  and  $I_C$ .

In this article, the optical constants of ZnS:Mn films deposited at different substrate temperatures were measured by SE. The band-gap energy of ZnS and the  ${}^4T_1(G) - {}^6A_1(S)$  transition energy of the doped  $\text{Mn}^{2+}$  ions as a function of deposition temperature were also investigated by optical transmittance and photoluminescence (PL) measurement, respectively. The observed changes in the optical properties of ZnS:Mn films are attributed to the phase transition between zinc-blende and wurtzite of the ZnS matrix due to different growth temperatures. This view is further substantiated by structural studies using x-ray diffractometry (XRD).

## II. EXPERIMENTAL DETAILS

Laser ablation of ZnS:Mn was carried out with an ArF excimer laser (Lambda Physik COMPex205, 193 nm, 20 ns) focused on a rotating target at an incidence angle of  $45^\circ$ . A laser fluence of  $\sim 2 \text{ J/cm}^2$  was used throughout the experiments. Deposition was performed in a vacuum chamber that was evacuated to a base pressure of  $1.5 \times 10^{-4}$  Torr and then backfilled with Ar to a pressure of 0.5 Torr. Films were grown on either (001)Si or ITO-coated glass substrates, which were mounted on a substrate holder with a resistive heater capable of heating the substrate up to  $500^\circ\text{C}$ . The substrate temperature was determined by a thermal coupled embedded directly underneath the substrate in the face plate of the substrate holder. The ZnS target used in this work was doped with 1% of Mn by weight. The distance between the substrate holder and the target surface was fixed at 4.5 cm.

Ellipsometric measurements were carried out by a spectroscopic phase modulated ellipsometer (Jobin Yvon UVISSEL) in the wavelength range of 350–850 nm at 5 nm intervals. All measurements were performed at a  $70^\circ$  angle of incidence with the analyzer and modulator set at  $45^\circ$  and  $0^\circ$ , respectively. The obtained spectra were best fitted using the double layer Sellmeier (DLS) model. The parameters, including the thickness of the films, obtained from each of the fittings were used to simulate  $n$  by the following dispersion relations:<sup>13</sup>

$$n^2 = A + B \times \frac{\lambda^2}{\lambda^2 - C^2}, \quad (5)$$

where  $n$  is the refractive index, and  $A$ ,  $B$ , and  $C$  are positive constants. Here,  $\lambda$  represents the wavelength ranging from 350 to 850 nm. Film thickness of our deposited films was also measured by a surface profiler (KLA-Tencor P-10) in order to cross check with our fitted thickness. Optical transmittance measurement was performed by an UV-VIS scanning spectrophotometer (Shimadzu UV-2101 PC). In our PL measurements, the ZnS:Mn films were excited by a 100 mW

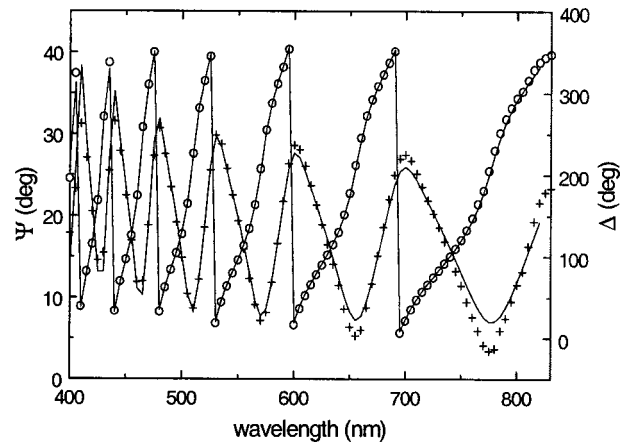


FIG. 1. Spectra of the ellipsometric parameters  $\psi$  and  $\Delta$  as functions of wavelength from SE experiments of ZnS:Mn film deposited at  $350^\circ\text{C}$ . The (+) and (○) are the measured  $\psi$  and  $\Delta$  values, respectively, while the solid lines are model fitting.

argon ion gas laser (Coherent Innova 70) operated in a single-wavelength mode at 488 nm. PL spectra were recorded by a double grating monochromator (SPEX 1403) equipped with a standard photon counting equipment. Finally, the crystallography of the as-grown ZnS:Mn films was studied by an x-ray diffractometer (Philips X'pert) using  $\text{Cu K}\alpha$  radiation.

## III. RESULTS

Dispersion curves of the two ellipsometric parameters,  $\psi$  and  $\Delta$ , for the ZnS:Mn film deposited on (001)Si at substrate temperature of  $350^\circ\text{C}$  is shown in Fig. 1. In general, all our ZnS films show similar oscillatory features due to their film thickness. Our initial analysis was based on a single layer Sellmeier model. Large discrepancy with the experimental data was obtained. In subsequent analysis, we modified the single layer Sellmeier model to a double layer Sellmeier (DLS) model. In this approach, we assume that the films consist of dual layers: a bottom bulk ZnS:Mn layer and a surface layer that composed of bulk ZnS:Mn as well as void. The void in the surface layer was mainly caused by surface roughness and porosity. Figure 2 shows the schematic diagram of the DLS model for our ZnS:Mn films. Based on this modified DLS model, excellent agreement with experimental data was obtained. The solid lines in Fig. 1 denote the fitted results of one of the films. A summary of the fitting param-

|                 |            |
|-----------------|------------|
| bulk ZnS + void | $d_s, n_s$ |
| bulk ZnS        | $d_b, n_b$ |
| (001) Si        |            |

FIG. 2. Schematic picture of the double layer Sellmeier (DLS) model.

TABLE I. Fitting parameters of ZnS:Mn films prepared at different deposition temperatures.

| $T(^{\circ}\text{C})$ | $A$  | $B$  | $C$   | $d_b$<br>(nm) | $d_s$<br>(nm) | Volume<br>fraction of<br>void $f(\%)$ | Thickness<br>measured by<br>surface<br>profiler<br>$d(\text{nm})$ |
|-----------------------|------|------|-------|---------------|---------------|---------------------------------------|---|
| 150                   | 3.46 | 1.73 | 278.9 | 699.5         | 22.9          | 37.2                                  | 720   |
| 250                   | 3.40 | 1.98 | 272.8 | 854.9         | 24.3          | 37.0                                  | 838   |
| 350                   | 3.31 | 2.05 | 267.7 | 556.3         | 27.6          | 34.2                                  | 504   |
| 450                   | 3.22 | 2.18 | 261.9 | 629.1         | 31.3          | 41.2                                  | 730   |

eters for all our ZnS:Mn films are listed in Table I. Based on the fitting parameters in Table I, we can see that the fitted film thicknesses,  $(d_s + d_b)$ , are close to those measured by the surface profiler ( $d$ ). Furthermore, both the  $d_s/d_b$  ratio and the volume fraction of void ( $f$ ) are smaller than those values obtained from sol-gel derived films,<sup>12</sup> reflecting the fact that PLD are, in general, smoother than sol-gel films. After securing the fitting parameters, the dispersion spectra of refractive index for the bottom layers,  $n_b$ , are evaluated using Eq. (5) and plotted in Fig. 3(a). Figure 3(b) shows the dependence of  $n_b$  at wavelength of 514 nm as a function of

deposition temperature. The Bruggeman effective medium approximation (EMA)<sup>14</sup> is used to describe the dispersion spectra of refractive index for the top ZnS:Mn layers, which is expressed by

$$(1-f) \frac{n_b^2 - n_s^2}{n_b^2 + 2n_s^2} + f \frac{1 - n_s^2}{1 + 2n_s^2} = 0, \quad (6)$$

where  $n_s$  is the effective refractive index of the surface layers. Figure 4 shows the  $n_s$  dispersion spectra as a function of growth temperature.

In general, the refractive indices  $n_s$  and  $n_b$  of the ZnS:Mn films are higher at shorter wavelength. Our results also reveal that the refractive index increases with growth temperature. For instant, when the deposition temperature is 150 °C, the refractive index  $n_b$  of the bottom ZnS:Mn layer is about 2.44 at 500 nm, while the corresponding value for the film grown at 450 °C is about 2.5. The rise of refractive index seems to be more pronounced for temperature range from 150 to 250 °C. It becomes less distinct between 250 and 450 °C. Similar temperature dependence is also observed in the  $n_s$  spectra. The escalation of  $n_b$  with deposition temperature may be a result of either changes in the structure (wurtzite and zinc-blende) or increase of film density. Further investigation of the effect of deposition temperature on the microstructure of the film using transmission electron microscope will be of importance. In order to estimate the surface roughness, we use the measured correlation of ellip-

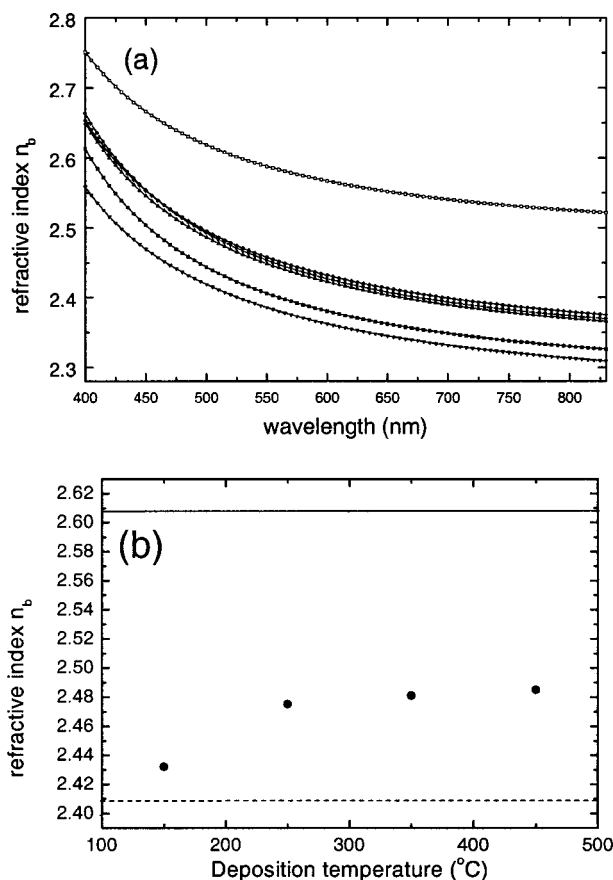


FIG. 3. (a) Refractive indices  $n_b$  of the bottom ZnS:Mn layers grown at 150 °C (—■—), 250 °C (—●—), 350 °C (—▲—), and 450 °C (—◆—). The dispersion curves for pure ZnS of wurtzite structure (—□—) and zinc-blende structure (—▼—) are also shown for Ref. 19. (b)  $n_b$  is plotted against deposition temperature at wavelength of 514 nm. The solid and dotted lines are the refractive indices of bulk ZnS of wurtzite and zinc-blende structures, respectively.

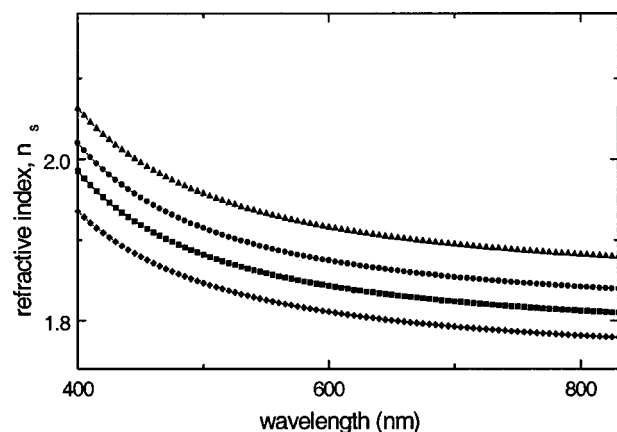


FIG. 4. Effective refractive indices  $n_s$  of the upper ZnS:Mn layers grown at 150 °C (—■—), 250 °C (—●—), 350 °C (—▲—), and 450 °C (—◆—) obtained by EMA.

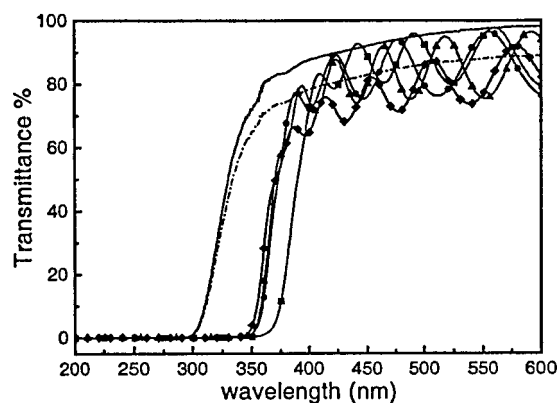


FIG. 5. Transmittance of ZnS:Mn films deposited on ITO-coated glass at 150 °C (—■—), 250 °C (—●—), 350 °C (—▲—), and 450 °C (—◆—). The transmittance spectra for ITO-coated glass before (—) and after (---) annealing at 500 mTorr of oxygen for 30 min are also shown for comparison.

sometry and atomic force microscopy (AFM) measurements of surface roughness obtained in  $a$ -Si<sub>1-x</sub>C<sub>x</sub>:H:<sup>15</sup>

$$d_s(SE) = 1.5R_q + 0.4 \text{ nm}, \quad (7)$$

where  $R_q$  is the surface roughness measured by AFM. We notice that our films have an estimated surface roughness between 15 and 21 nm. This value is typical for PLD films of about several hundred nanometers thick.

Figure 5 shows the transmittance of ZnS:Mn films grown on ITO-coated glass at different deposition temperatures. All films show good optical transmittance of  $\sim 80\%$  in the visible region. The transmittance, however, is slightly reduced to  $\sim 70\%$  as the deposition temperature is raised to 450 °C. The measured transmittance spectra of ITO-coated glass are also shown in the figure for comparison. Obviously, the absorption edges at  $\sim 300$  and  $\sim 350$  nm are originated from ITO and ZnS, respectively. For films deposited at 150 °C, the absorption edge of ZnS is located at  $\sim 370$  nm. As the deposition temperature is increased, this absorption edge shifts to shorter wavelength. This shift is more or less the same for films grown at 250–450 °C. In the figure, the absorption spectra of the ITO-coated glass before and after annealing at 450 °C are also shown for reference. Apparently, the shift of the absorption edges from 370 to 350 nm is not related to the ITO-coated glass substrates. For direct band-gap transition, the relation between the absorption coefficient  $\alpha$  and the energy of the incident light  $h\nu$  is given by:<sup>6,16,17</sup>

$$(\alpha h\nu)^2 = B(h\nu - E_g), \quad (8)$$

where  $B$  is a constant and  $E_g$  is the band-gap energy. Figure 6 shows the plot of  $(\alpha h\nu)^2$  as a function of  $h\nu$ . By extrapolating the linear portion of the curve to zero, band-gap energies of 3.5, 3.47, 3.44, and 3.28 eV are obtained for our films deposited at 450, 350, 250, and 150 °C, respectively. They are all lower than that of bulk ZnS. As the band-gap energy is not likely dependent on the density of ZnS:Mn films, the change in refractive index and band-gap energy with deposition temperature might not relate to the change in the film density. On the other hand, the band-gap energy of ZnS is

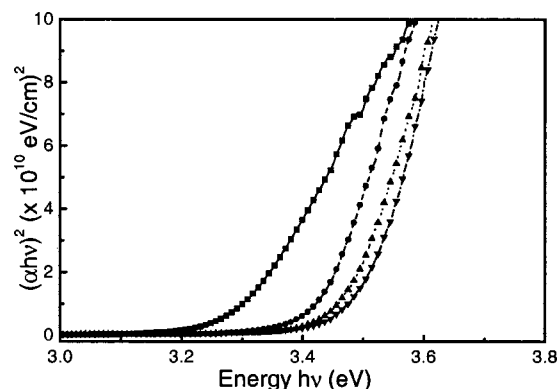


FIG. 6. Profiles of  $(\alpha h\nu)^2$  against  $h\nu$  for ZnS:Mn films deposited at 150 °C (—■—), 250 °C (—●—), 350 °C (—▲—), and 450 °C (—◆—).

known to depend on its crystalline structure. The band-gap energies of zinc-blende and wurtzite ZnS at room temperature are 3.66 and 3.82 eV, respectively.<sup>18</sup> This indicates that the change of the measured band-gap energies in our samples may be due to change in the ZnS structure. Indeed, at a low deposition temperature of 150 °C, the films consist mainly of zinc-blende structure. They exhibit a lower refractive index and a lower band gap energy. At higher deposition temperatures, the films possess a higher wurtzite to zinc-blende ratio and give rise to a wider band gap and a larger refractive index. Therefore, the shifts of both the absorption edge and band-gap energy are caused by the change of wurtzite to zinc-blende ratio in the ZnS:Mn films under different growth temperatures.

Figure 7 shows the PL spectra of the films deposited on (001)Si at 150 and 450 °C. The PL spectra show an orange-yellow emission band at  $\sim 590$  nm, which is due to the  ${}^4T_1(G) - {}^6A_1(S)$  transition of the Mn<sup>2+</sup>.<sup>8</sup> At increased deposition temperatures, the PL band becomes narrower and shifts to shorter wavelength. The inset shows the peak position of this PL band as a function of deposition temperature. The peak position also shows a larger shift at the 150–250 °C range. Therefore, we believe that the change in the PL spectra may have the same origin as that observed in the SE and transmittance spectra. Indeed, the crystal-field splitting of the 3d<sup>5</sup> electron configuration of Mn<sup>2+</sup> in host

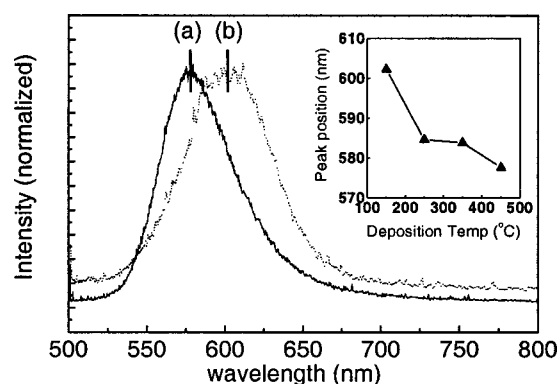


FIG. 7. PL spectra of ZnS:Mn films deposited on (001)Si at (a) 450 °C and (b) 150 °C. Inset is the peak position of the PL band as a function of deposition temperature.



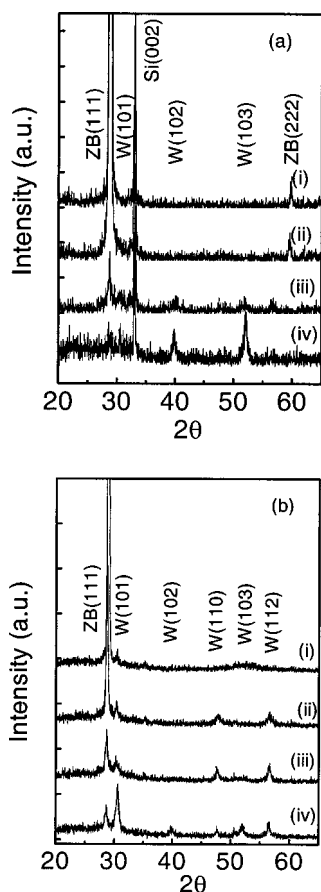


FIG. 8. XRD patterns of the ZnS:Mn films grown on (a) (001)Si with deposition temperature of (i) 150 °C, (ii) 250 °C, (iii) 350 °C, and (iv) 450 °C; on (b) ITO-coated glass with deposition temperatures of (i) 150 °C, (ii) 250 °C, (iii) 350 °C, and (iv) 450 °C.

matrices of crystal symmetry is different. Hence the energy in the transition of  ${}^4T_1(G) - {}^6A_1(S)$  of  $Mn^{2+}$  ions could be different in zinc-blende ZnS and wurtzite ZnS. A similar shift has also been reported for the EL emission band from ZnS:Mn films.<sup>11,18</sup>

Figure 8(a) shows the XRD patterns of ZnS:Mn films grown on (001)Si at different deposition temperatures. At a low deposition temperature of 150 °C, only diffraction peaks of zinc-blende ZnS are observed. For films grown at higher temperatures, peaks of wurtzite structure appear. As a result, the films contain a mixture of zinc-blende and wurtzite structures. Similar structural changes at different deposition temperatures are also observed for ZnS:Mn films grown on ITO-coated glass as shown in Fig. 8(b). Hence, our XRD results illustrate the structural variation of the ZnS:Mn films and support our interpretation of the measured optical data.

#### IV. CONCLUSIONS

ZnS:Mn films were successfully deposited on (001)Si and ITO-coated glass by PLD method. The optical dispersion functions of the ZnS:Mn films grown at different deposition temperatures were obtained by spectroscopic ellipsometry. A more accurate estimation of the optical constant of the ZnS:Mn films was achieved by a modified double layer Sellmeier model, in which an effective surface layer representing the surface roughness was introduced. The refractive indices of the ZnS:Mn films were seen to increase with deposition temperature. Shifts in the absorption edge, band-gap energy and PL emission band due to different film growth temperatures were also observed. All these changes in the optical properties of the ZnS:Mn films are correlated with the structural variations of the films.

#### ACKNOWLEDGMENTS

The authors would like to thank W. L. Tsui for his helpful discussion. The work described in this article was supported by the Center for Smart Materials of the Hong Kong Polytechnic University (under Grant No. A316). K.M.Y. and W.S.T. were supported by MPhil studentships of the Hong Kong Polytechnic University.

- <sup>1</sup>S. K. Mandal, S. Chaudhuri, and A. K. Pal, *Thin Solid Films* **350**, 209 (1999).
- <sup>2</sup>J. Fang, P. H. Holloway, J. E. Yu, and K. S. Jones, *Appl. Surf. Sci.* **70/71**, 701 (1993).
- <sup>3</sup>K. Uchino, K. Ueyama, M. Yamamoto, H. Kariya, H. Miyata, H. Misasa, M. Kitagawa, and H. Kobayashi, *J. Appl. Phys.* **87**, 4249 (2000).
- <sup>4</sup>C. T. Hsu, *Thin Solid Films* **335**, 284 (1988).
- <sup>5</sup>W. Tang and D. C. Cameron, *Thin Solid Films* **280**, 221 (1996).
- <sup>6</sup>B. Elidrissi, M. Addou, M. Regragui, A. Bougrine, A. Kachouane, and J. C. Bernède, *Mater. Chem. Phys.* **68**, 179 (2001).
- <sup>7</sup>R. H. Mauch, *Appl. Surf. Sci.* **92**, 589 (1996).
- <sup>8</sup>W. P. Shen and H. S. Kwok, *Appl. Phys. Lett.* **65**, 2162 (1994).
- <sup>9</sup>M. McLaughlin, H. F. Sakeek, P. Maguire, W. G. Graham, J. Molloy, S. Lavery, and J. Anderson, *Appl. Phys. Lett.* **63**, 1865 (1993).
- <sup>10</sup>S. Richter and R. H. Mauch, *J. Appl. Phys.* **83**, 5433 (1998).
- <sup>11</sup>Y. A. Ono, in *Electroluminescent Displays* (World Scientific, Singapore, 1995), pp. 82–83.
- <sup>12</sup>C. L. Mak, B. Lai, K. H. Wong, C. L. Choy, D. Mo, and Y. L. Zhang, *J. Appl. Phys.* **89**, 4491 (2001).
- <sup>13</sup>T. M. Bieniewski and S. J. Czyzak, *J. Opt. Soc. Am.* **53**, 496 (1963).
- <sup>14</sup>D. A. G. Bruggeman, *Ann. Phys. (Leipzig)* **24**, 636 (1935).
- <sup>15</sup>J. Koh, Y. Lu, C. R. Wronski, Y. Kuang, R. W. Collins, T. T. Tsong, and Y. E. Strausser, *Appl. Phys. Lett.* **69**, 1297 (1996).
- <sup>16</sup>T. He, P. Ehrhard, and P. Meuffels, *J. Appl. Phys.* **79**, 3219 (1995).
- <sup>17</sup>C. H. Kam, S. D. Cheng, Y. Zhou, K. Pita, X. Q. Han, W. X. Que, H. X. Zhang, Y. L. Lam, Y. C. Chan, Z. Sun, and X. Shi, *Proc. SPIE* **3896**, 466 (1999).
- <sup>18</sup>H. Yamamoto, in *Zinc Sulphide, Luminescence and Related Properties of II-VI Semiconductors*, edited by D. R. Vij and N. Singh (NOVO Science, 1998), p. 202.
- <sup>19</sup>M. Bass, E. W. Stryland, D. R. Williams, and W. L. Wolfe, *Handbook of Optics* (McGraw-Hill, New York, 1995), Vol. II. p. 33.67.